

## Predicting the preferred morphology of hexagonal boron nitride domain structure on nickel from ReaxFF-based molecular dynamics simulations

Song Liu<sup>1</sup>, Jeffrey Comer<sup>2</sup>, Adri C.T. van Duin<sup>3</sup>, Diana M. van Duin<sup>3</sup>, Bin Liu\*<sup>1</sup>, James H. Edgar\*<sup>1</sup>

<sup>1</sup>Department of Chemical Engineering, Kansas State University, Manhattan, KS 66506

<sup>2</sup>Department of Anatomy and Physiology, Kansas State University, Manhattan, KS 66506

<sup>3</sup>RxFF\_Consulting LLC, State College, PA 16801

**Corresponding authors:** binliu@ksu.edu, and edgarjh@ksu.edu

**Fig. S1.** Energies of triangular hBN on Ni(111) from periodic DFT calculations as a function of the total edge length (3L).

**Fig. S2.** Energies of hexagonal hBN, bounded by zigzag edges, on Ni(111) from periodic DFT calculations as a function of the total edge length (3L).

**Fig. S3.** Edge energies of B- and N-terminated triangular and hexagonal hBN domains with zigzag edge configurations on Ni(111).

**Fig. S4** Counts of hexagons in the hBN domains obtained from MD simulations over 10 ns at B:N = 3:1 (orange), 2:1 (blue), 1:1 (grey), 1:2 (red), 1:3 (purple), and 1:4 (green).

**Fig. S5** Thermodynamic cycle for N<sub>2</sub> formation at the Ni(111) surface. The formation of N<sub>2</sub>(g) from atomic N adsorbed on Ni(111) is described by eqn (1) in the main text.

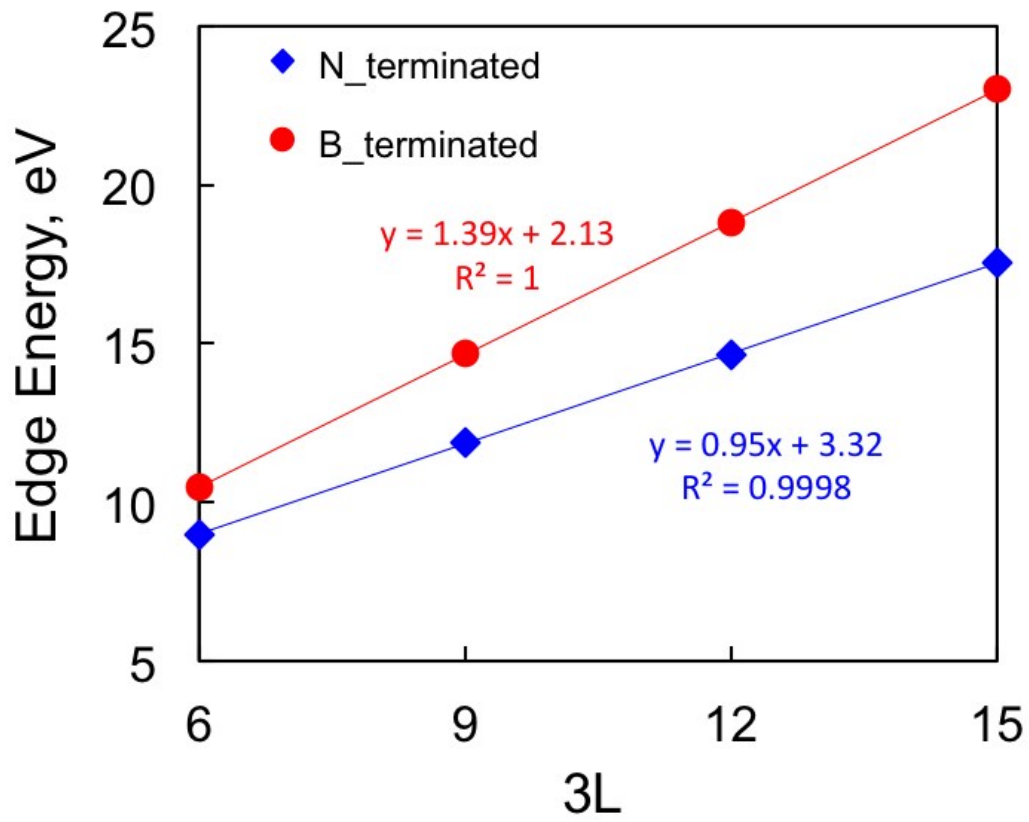


Fig. S1

Liu et al.

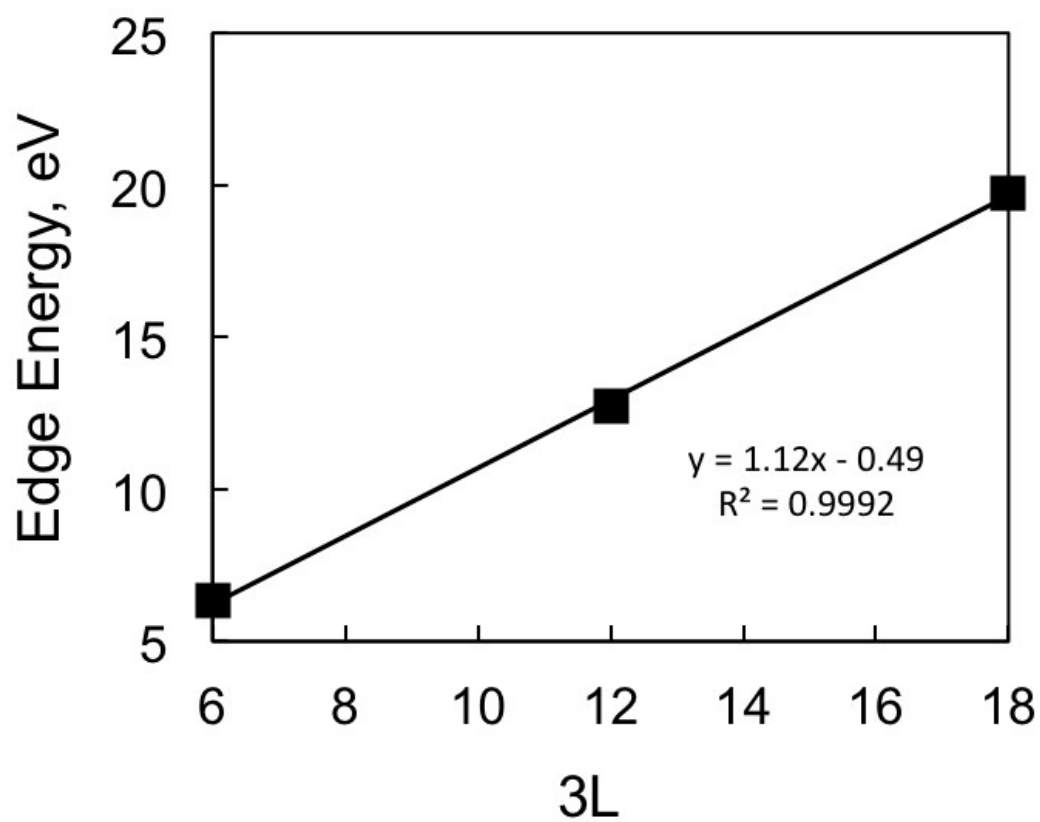


Fig. S2

Liu et al.

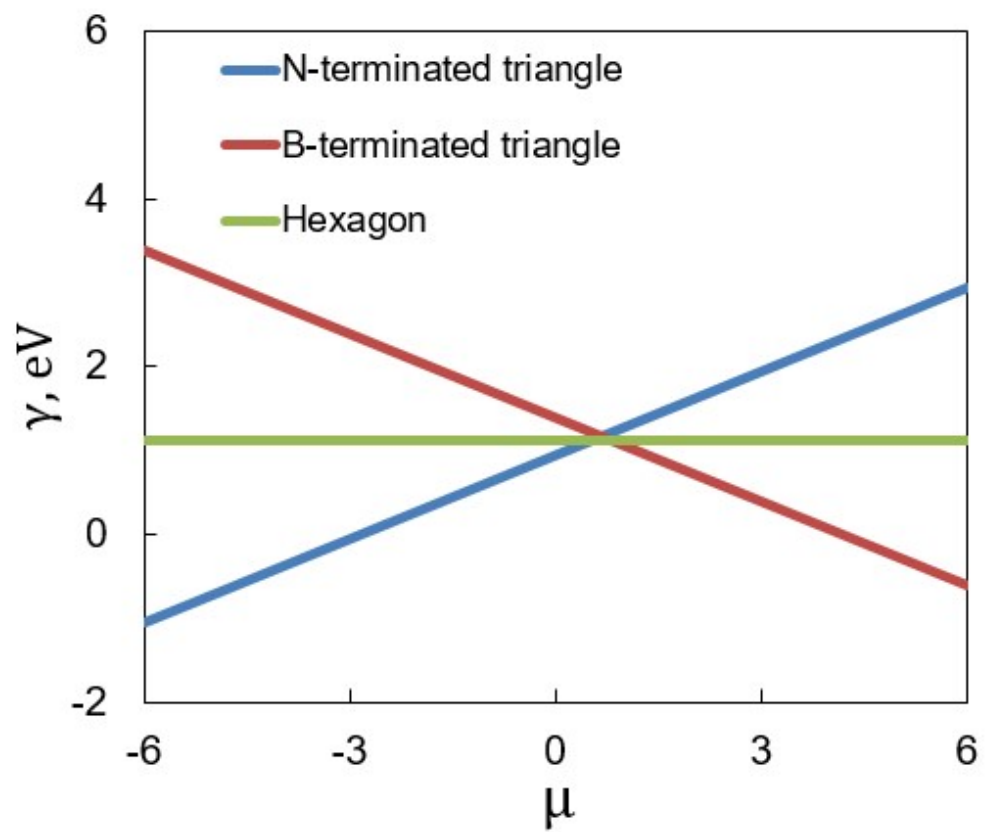


Fig. S3

Liu et al.

**Computational details for triangular and hexagonal hBN edge energy calculations.** The edge energies ( $\gamma_{ZB}$  and  $\gamma_{ZN}$ ) of triangular hBN on Ni(111) can be described by Equations (S1) and (S2), as discussed by Yakobson and coworkers [1].

$$\gamma_{ZB} = \frac{E_T - E_{Ni} - M_{BN}\mu_{BN} - \mu_B - L\mu_B}{3L} = \gamma_{ZB}^* - \frac{\mu}{3} \quad (\text{S1})$$

$$\gamma_{ZN} = \frac{E_T - E_{Ni} - M_{BN}\mu_{BN} - \mu_N - L\mu_N}{3L} = \gamma_{ZN}^* + \frac{\mu}{3} \quad (\text{S2})$$

where  $E_T$  and  $E_{Ni}$  are the total energies of adsorbed hBN and clean Ni(111), respectively.  $M_{BN}$  is the number of BN pairs in each hBN domain.  $\mu_{BN}$ ,  $\mu_B$ , and  $\mu_N$  are defined as the chemical potentials of the BN pair, and elemental B, N species in an infinite hBN monolayer, respectively. We let  $\mu_{BN}$ ,  $\mu_B$ , and  $\mu_N$  obey the relationships, following Equations (S3) and (S4).

$$\mu_{BN} = \mu_B + \mu_N, \quad (\text{S3})$$

$$\mu_{B/N} = \frac{1}{2}\mu_{BN} \pm \mu, \quad (\text{S4})$$

and

where  $\mu$  in Equation (S4) represents an arbitrary parameter which can be used to tune the chemical potentials of B and N species. By letting  $\mu = 0$ ,  $\gamma_{ZN}^* = 1.39 \text{ eV}$  and  $\gamma_{ZB}^* = 0.95 \text{ eV}$ .

For hexagonal hBN domains on Ni(111), the edge energy ( $\gamma_Z$ ) is defined by Equation (S5), which is independent of  $\mu$ . The edge energies for the geometries in Figure 1(c) also show a strict linear relationship with the edge length L (see Figure S2).

$$\gamma_Z = \frac{E_T - E_{Ni} - M_{BN}\mu_{BN}}{6L} \quad (\text{S5})$$

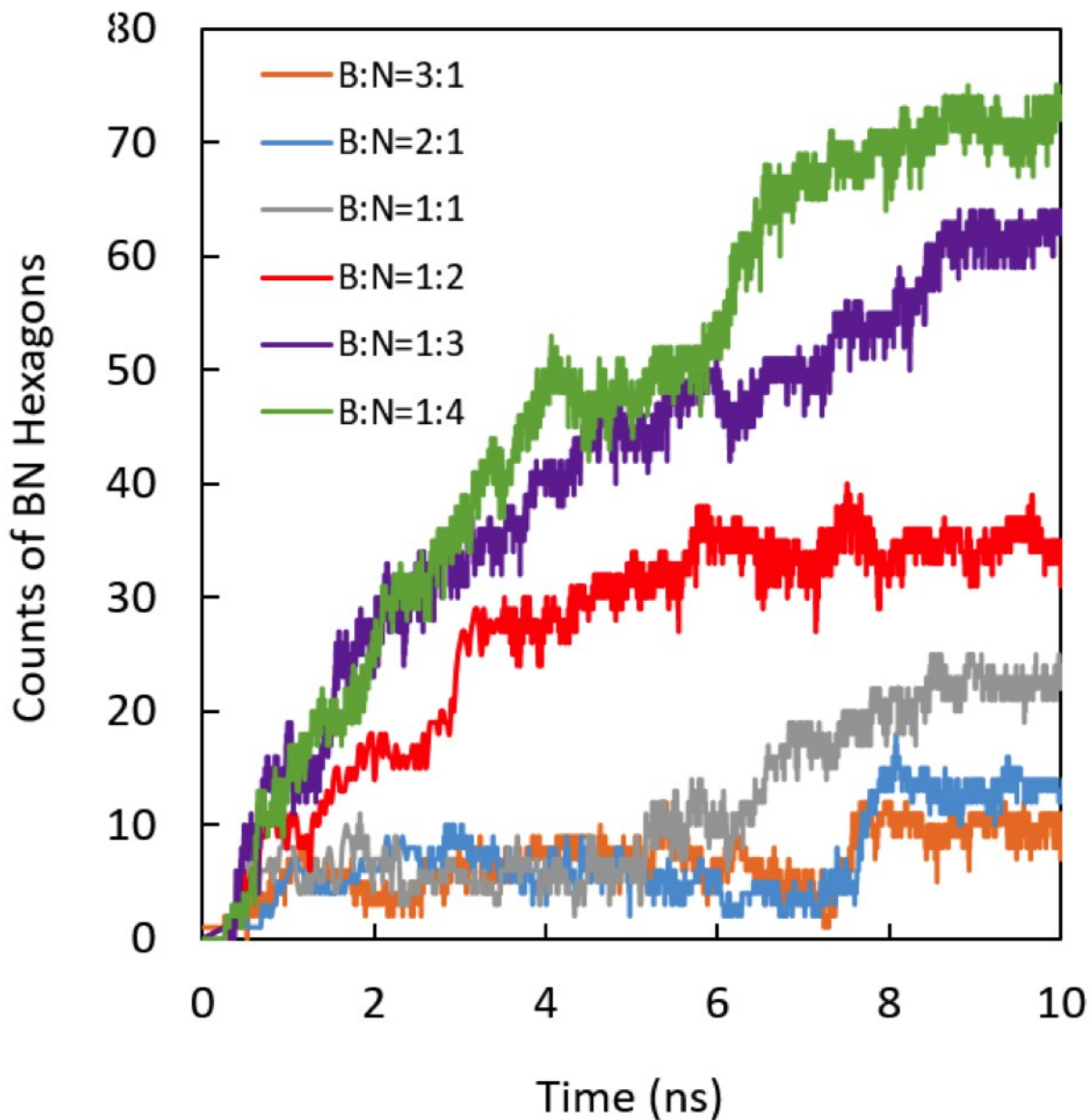


Fig. S4

Liu et al.

As shown in Fig. S4, at B:N = 3:1 (orange) and 2:1 (blue), the number of BN hexagons grew more slowly - only five hexagons formed in the first 7 ns, most of which were formed in the initial period (within the 1<sup>st</sup> ns). The numbers of BN hexagons finally reached approximately 10 counts in both cases at around 8 ns. At the stoichiometric B:N ratio (grey), the initial growth is at a similar pace (in the first 6 ns) to those at B-rich conditions. However, the number of BN hexagons nearly doubled and reached a count of 22 in the next 4 ns. The slow growth at the initial stage suggests that growth is limited by the arrival of sufficient nitrogen; nitrogen is the

rate-limiting species. Under nitrogen-lean and stoichiometric conditions, an induction period is required before the growth occurs. At B:N = 1:2 (yellow), the growth rate in BN hexagon counts grew at much faster rates, with more than 15 counted after 2 ns of MD run. At the 3<sup>rd</sup> ns, the number of BN hexagon increased significantly, reaching 27. During the remaining 7 ns, the number of BN hexagon grows at a slower pace and eventually reached approximately 30. The slower growth after 3 ns can be attributed to the depletion of nitrogen and boron sources. As shown in Figure 4 (a)(in purple and green), 64 and 75 hexagons formed by 10 ns, respectively. At the early stage (in the first 2 ns), the number of BN hexagons grew at a pace of 15 hexagons/ns. The main difference between simulations performed at nitrogen excess conditions is that at, B: N = 1:4, the domain growth outpaces that at B:N = 1:3 after 6 ns.

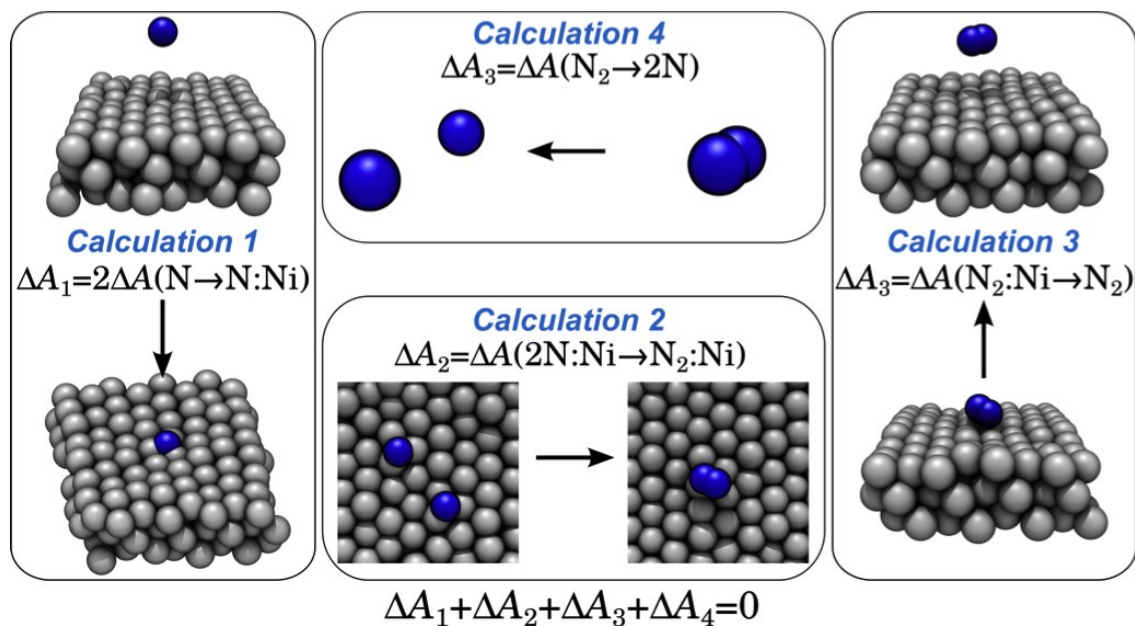


Fig. S5

Liu et al.

**Free energy calculations for N<sub>2</sub> dissociation thermodynamic cycle.** To characterize the complete thermodynamics of N<sub>2</sub> formation from atomic N and adsorption on the Ni(111), we performed four different free energy calculations, which are illustrated in Fig. S5. For calculations of the adsorption/desorption free energy of atomic N (Calculation 1) and N<sub>2</sub> (Calculation 3), we defined the transition coordinate,  $Z$ , as the  $z$ -projection of the vector between the centre of mass of all Ni atoms and the centre of mass of N atoms. The adaptive biasing force method was applied to this coordinate using bins of size of 0.05 Å in a domain of  $4.2 \text{ \AA} \leq Z \leq 10.0 \text{ \AA}$ . Because the interaction between atomic N and Ni is strong (with a binding energy of 1.26 eV), restraints (a flat-bottomed harmonic potential) were imposed in step 3 on each Ni atom at  $z > 4.0 \text{ \AA}$  to prevent them from leaving the upper layer during Ni–N bond separation. It is important to point out that these restraints were not active at the endpoints of the calculation ( $Z = 3.05 \text{ \AA}$ , where N was fully adsorbed; and  $Z > 8 \text{ \AA}$ , where the N atom and the surface were fully separated). Hence, the change in free energy between the fully adsorbed and fully dissociated states was rigorously obtained from Calculation 3. The calculations details for N<sub>2</sub> dissociation and association, to complete this thermodynamic cycle, are explained in the main text.



**References:**

(1) S. Liu, A.C.T. van Duin, D.M. van Duin, B. Liu, J.H. Edgar, "Atomistic Insights into Nucleation and Formation of Hexagonal Boron Nitride on Nickel from First-Principles-Based Reactive Molecular Dynamics Simulations", *ACS Nano*, 11 (2017) 3585-3596.